有机化学 DOI: 10.6023/cjoc202211030 研究论文
Chinese Journal of Organic Chemistry ARTICLE

一种三苯胺基二氟硼发光化合物的力致可逆荧光变色及数据安全保护研究

徐茂财[†,a] 田佳壮[†,a] 杨艳华*[,a] 苟高章*[,b]
李福敏[c] 邵 林*[,d] 池可心[e]

([a]昆明学院化学化工学院 云南省金属有机分子材料与器件重点实验室 昆明 650214)
([b]红河学院化学与资源工程学院 云南省天然药物与化学生物学重点实验室 云南蒙自 661100)
([c]大理州食品检验检测院理化检验中心 云南大理 671100)
([d]大理州食品检验检测院色谱分析中心 云南大理 671100)
([e]上海爱博才思分析仪器贸易有限公司 上海 200335)

摘要 为了满足信息快速发展对数据存储安全的要求，设计并成功合成了一种 π-共轭三苯胺基二氟硼化合物(**PyTPABF$_2$**). **PyTPABF$_2$** 具有正的溶剂化变色行为、分子内电荷转移性质、聚集诱导发射行为和高对比度机械荧光性能. 在外部机械刺激和有机溶剂熏蒸下，所制备的 **PyTPABF$_2$** 粉末的荧光颜色可在绿色和卡其色间可逆转变，这一现象源于晶态和无定形之间的相变过程. 更重要的是，基于 **PyTPABF$_2$** 的数据安全纸可以实现信息的可重写存储，有助于智能发光材料的合理设计.

关键词 三苯胺基二氟硼化合物；机械荧光行为；数据安全保护

Reversible Mechanofluorochromic and Data Security Protection of a Triphenylamine-Based Difluoroboron Luminescent Compound

Xu, Maocai[†,a] Tian, Jiazhuang[†,a] Yang, Yanhua*[,a] Gou, Gaozhang*[,b]
Li, Fumin[c] Shao, Lin*[,d] Chi, Kexin[e]

([a] *Yunnan Key Laboratory of Metal-Organic Molecular Materials and Device, School of Chemistry and Chemical Engineering, Kunming University, Kunming 650214*)
([b] *Key Laboratory of Natural Pharmaceutical & Chemical Biology of Yunnan Province, School of Chemistry and Resources Engineering, Honghe University, Mengzi, Yunnan 661100*)
([c] *Physical and Chemical Inspection Center, Dali Institute for Food Control, Dali, Yunnan 671100*)
([d] *Chromatographic Analysis Center, Dali Institute for Food Control, Dali, Yunnan 671100*)
([e] *Shanghai AB SCIEX Analytical Instrument Trading Co., Shanghai 200335*)

Abstract In order to meet the demand of data storage security in the rapid development of information, a π-conjugated triphenylamine-based difluororboron compound (**PyTPABF$_2$**) was designed and successfully synthesized. **PyTPABF$_2$** held positive solvatochromism behavior, intramolecular charge transfer property, aggregation-induced emission behavior and high contrast mechanofluorochromic performance. The as-prepared powders **PyTPABF$_2$** exhibited bright green fluorescence (533 nm), which luminescent color switching to khaki (556 nm) under external mechanical stimulation, meanwhile, the color could recover to original state after fuming. The X-ray diffraction (XRD) measurement demonstrated that this phenomenon originated from the process of phase transformation between crystalline and amorphous. More importantly, **PyTPABF$_2$**-based data secu-

* Corresponding authors. E-mail: yh_yangkmu@126.com; hhxylxyhxx@126.com; 631941087@qq.com
Received November 25, 2022; revised February 1, 2023; published online March 17, 2023.
Project supported by the Innovation and Entrepreneurship Training Program for University Students in Yunnan Province (No. 202111393026), the Basic Research Programs of Yunnan Science and Technology Department (No. 202101AU070060), the Research Foundation for Introduced Talents of Kunming University (No. YJL2008) and the First-rate Undergraduate Major Construction Project of Chemistry in Yunnan Province.
云南省大学生创新创业计划训练(No. 202111393026)、云南省科技厅基础研究(No. 202101AU070060)、昆明学院人才引进计划(No. YJL2008)和云南省一流本科专业建设专项资助项目.
† 共同第一作者(These authors contributed equally to this work).

rity paper could be achieved rewritable storage of information. It was of assistance in the rational design of smart luminescent materials.

Keywords triphenylamine-based difluororboron compound; mechanofluorochromic behavior; data security protection

1 Introduction

With the rapid development of information technology, data-security protection in the field of information encryption and decryption has attracted an enormous amount of attention.[1-2] And the development of ink-free rewritable paper has become one of the hotspots of current research. In order to meet the needs of information storage and security, Qin and Tang *et al.*[3] designed two electrofluorochromic polymers, the devices of ITO/polymers/gel electrolyte/ITO exhibited a high capacity storage and multilevel anti-counterfeiting capability under applied voltage stimulation. Yan *et al.*[4] reported 9,10-azaboraphenanthrene-based viologens could be realized a reversible data encryption through redox processes switching on/off states under electro-stimiltaneous. Compared with electrofluorochromic materials, mechanofluorochromic (MFC) organic compounds were more convenient operation, more affordable, and faster data writing and erasing processes.

MFC is a phenomenon that luminescence color of solid or crystalline could be switched under external mechanical stimulation, including grinding and crushing *etc*. Not only that, the fluorescence emission wavelength and emitting color of the most of MFC materials could recover original state by fuming or heating. In recent years, a considerable number of researches have been implemented in the field of MFC materials for ink-free rewritable paper. In general, MFC materials with aggregation-induced emission (AIE) property, including tetraphenylethylene functionalized 1,4-dihyfropyrrolo[3,2-*b*]pyrrole,[5] vinamidinium salts,[6] phenothiazine derivative,[7] naphthalene-based compound,[8] cationic Ir(III) complexes[9] and difluoroboron compounds and so on, had been reported to have potential application in security printing and data storage. Especially, difluoroboron compounds possessed fascinating optical features and tunability of optical behaviors as solid-state luminescent materials by reasonable chemical modification under the stimulation of external forces, which had sparked tremendous interests due to unique photophysical performance.[10-13] And BF_2-core moiety was usually used as electron-acceptor due to the vacant *p*-orbital on the boron center.[14] Above all, constructing an electron-donor and electron-acceptor (D-A) molecular system was a matter of prime importance. Then AIE activity was further study, and MFC materials with obvious luminescence color difference were selected to explore data-security protection performance.

Based on this consideration, a D-π-A conjugated molecule, **PyTPABF$_2$**, including triphenylamine group as the electron donating section and difluororboron unit as the electron accepting moiety was designed and prepared. Optical performance test displayed that **PyTPABF$_2$** not only possessed positive solvatochromism behavior in organic solvents of different polarity, but also had AIE-activity in THF/water mixtures. Further studies showed that the as-prepared powders of **PyTPABF$_2$** emitted bright green light (533 nm), however, luminescence color switched to khaki (556 nm) under external mechanical stimulation, and color could recover to original state after fuming using CH_2Cl_2 vapor. Such a significant color change, **PyTPABF$_2$** was used for data security detection research. XRD pattern in different solid state illustrated that the process of crystalline to amorphous transition was responsible for MFC behavior.

2 Results and discussion

2.1 Molecular synthesis and characterization

The synthetic route of **PyTPABF$_2$** was depicted in Scheme 1. Firstly, amide compound **PyBr** was prepared using commercial 2-amino-4-bromopyridine reaction with indole-2-carboxylic acid methyl ester, then it underwent Suzuki coupling reaction to synthesize **PyTPA**. Finally, **PyTPABF$_2$** was obtained using **PyTPA** reaction with BF_3•OEt_2 in the presence of NEt_3 by coordination reaction. In the process, the NH moieties of pyrrole and amide both

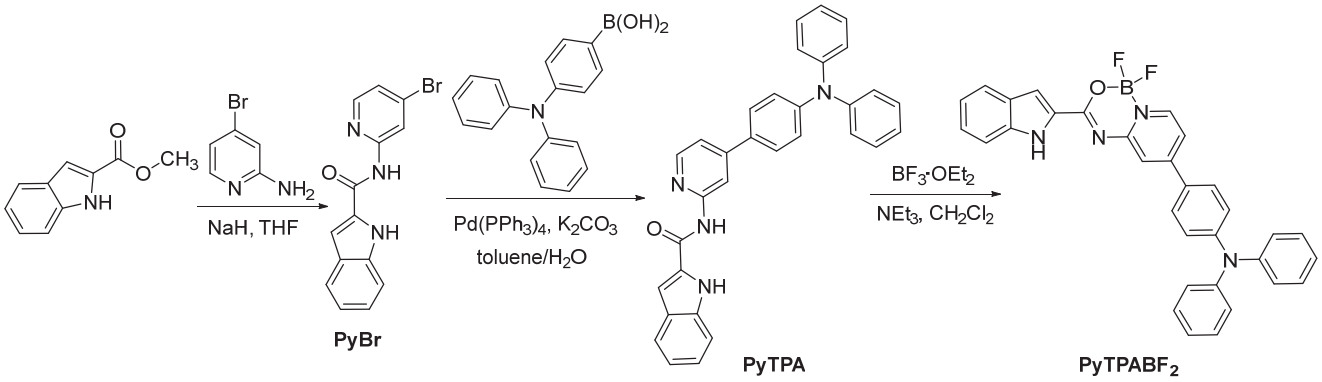

Scheme 1 Synthetic route of **PyTPABF$_2$**

were active sites, nevertheless, amide NH unit had better chemical reactivity.[15] ^{1}H NMR spectra was used to confirm this conjecture. As shown in Figure 1, the signals of pyrrole NH group appeared about δ 12, the signals of amide NH group were located around δ 11, which appearing in compound **PyBr** and keeping in precursor **PyTPA**, disappearing in complex **PyTPABF$_2$**. It suggested that a formed site of BF_2-core was seated around amide and pyridine moieties. And the chemical shifts of α_H, β_H and γ_H in pyridine group were also found, there were some differences in signal positions due to the influence of charge characteristics of compounds.

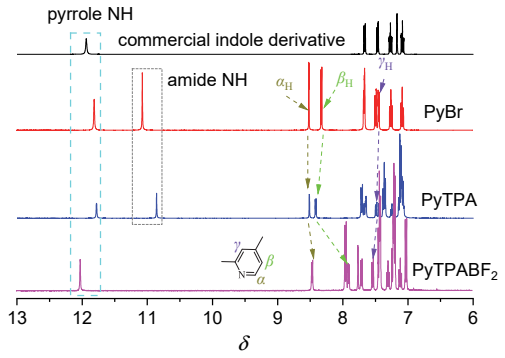

Figure 1 Overlay plots of ^{1}H NMR spectra

2.2 UV-vis absorption and fluorescent emission spectra in solutions

The solvatochromism of **PyTPABF$_2$** was experimented. As shown in Figure 2, there were two main absorption bands located at approximately 300 and 400 nm, respectively.

The former was attributed to π-π* transition, the latter was ascribed to intramolecular charge transfer from tripenylamine group as the electron donor to difluoroboron unit as the electron acceptor. Among them, the maximum absorption wavelength (λ_{max}) was located at 406, 414, 415, 407, 415 and 418 nm in different polarity organic solvent, respectively, originating from $S_{0,0}$-$S_{1,0}$ transition according to the Laporte's parity selection rule,[16] and molar extinction coefficient (ε) was calculated to 2.17, 3.04, 2.91, 2.60, 2.67 and 3.26×10^4 L•mol^{-1}•cm^{-1}. Meanwhile, a shoulder peak was observed at 375, 379, 374, 372, 380 and 380 nm, coming from $S_{0,0}$-$S_{1,1}$ transition. Furthermore, π-π* transition band also had two absorption peaks, which mainly absorption peak wavelength was located at about 290 nm and smaller absorption peak was located at around 305 nm, suggesting that **PyTPABF$_2$** had a vibrational fine structure in organic solvents. On the whole, the λ_{max} values were almost unchanged with increasing of solvent polarity, indicating that the dipole moment between the equilibrium ground and the Frank-Condon excited states was little difference.[17]

However, the solvent effect of **PyTPABF$_2$** in organic solvents of different polarity was evidently observed. As shown in Figure 2(b), the emission wavelengths were gradually red-shifted, which emitting different colors light

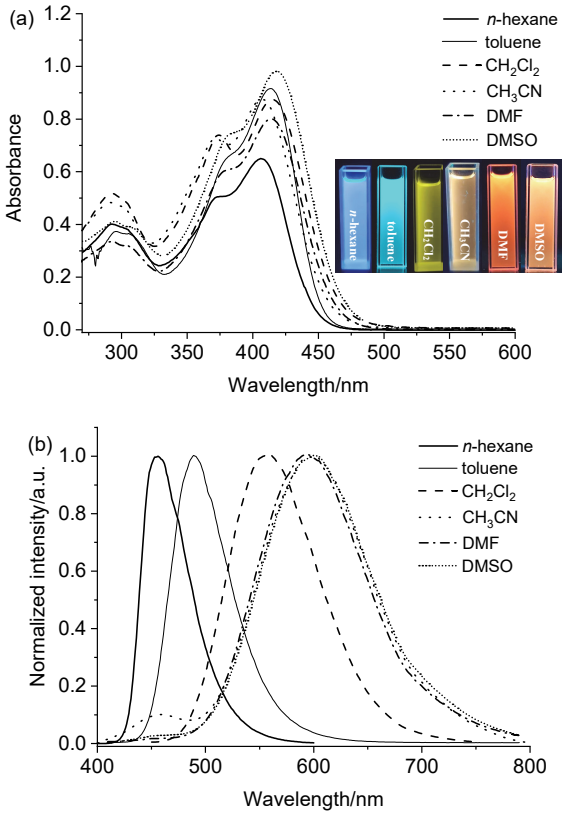

Figure 2 (a) UV-vis absorption spectra and (b) normalized fluorescence emission spectra of **PyTPABF$_2$** in different solvents
Inset: photos in different solvents irradiation 365 nm

under 365 nm irradiation. Meanwhile, the dual emission could be observed in CH_3CN. The shorter and longer wavelength were located at 460 and 597 nm, originating from the locally excited (LE) and twisted intramolecular charge transfer (TICT) states, respectively. These results indicated that **PyTPABF$_2$** possessed ICT property and positive solvatochromism behavior.

2.3 Theoretical calculation

To better explain the observed photophysical behaviors of **PyTPABF$_2$**, molecular simulations were performed after optimizing structure to the lowest energy conformation from the density functional theory (DFT) using M062X functional with 6-31G(d) as the basic set through the Gaussian 09 program package. As shown in Table 1, in the ground state and excited state, the electron density distribution of the highest occupied molecular orbital (HOMO) was mainly located on the donor TPA section, whereas that of the lowest unoccupied molecular orbital (LUMO) was distributed around the acceptor BF_2-core moiety. And the HOMO−1 had a largest overlapping zone with the LUMO. Such separated electron density distribution indicated that CT process could occur from the electron donor to the electron acceptor.

The energy barriers were 5.12 and 5.43 eV from the HOMO and HOMO−1 to LUMO, respectively. Therefore, the charges on the HOMO and HOMO−1 were excited to the LUMO, respectively, rather than the HOMO−1 to

Table 1 Calculated spatial distributions and optimized conformation of **PyTPABF$_2$** in ground and excited states

Frontier orbital	Ground state		Excited state	
	Electron density distribution	Energy level	Electron density distribution	Energy level
LUMO+1	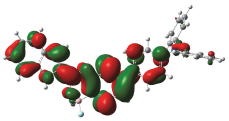	−0.94 eV	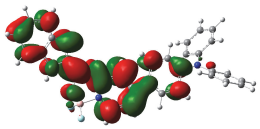	−1.07 eV
LUMO	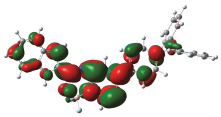	−1.66 eV	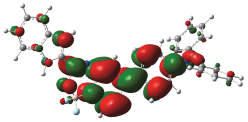	−2.05 eV
HOMO	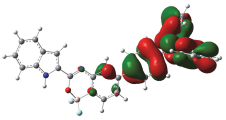	−6.78 eV	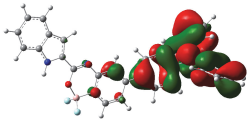	−6.72 eV
HOMO−1	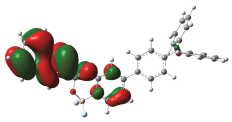	−7.09 eV	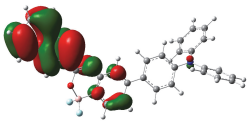	−7.07 eV

LUMO+1 (6.15 eV of energy barriers) in the ground state. In the excited state, the energy barriers were 4.67 and 5.02 eV from the HOMO and HOMO−1 to LUMO, respectively. It was smaller than that of the ground state, indicating that the excited state was more conducive to CT processes (Table 2). The dihedral angles between indole unit and BF_2-core, coordinated pyridine group and phenyl of TPA moiety in the excited state were smaller than that of the ground state. Furthermore, TPA group possessed a propeller-shaped geometry, which means that TPA group inherently had a twisted molecular conformation.[18-20] It demonstrated that the molecular conformation of the excited state was more distorted, which was beneficial to TICT process. The above results indicated that **PyTPABF$_2$** molecule was provided with a distorted molecular spatial configuration, which considerably reduced close packing in solid state and was conducive to MFC behavior.

To better understand the shorter wavelength of dual emission in CH_3CN as the LE fluorescence, molecular simulation on the ground state and the lowest singlet excited state were performed. As shown in Table 3, the hole was mainly delocalized on the TPA and indole moieties for the transition from S_0 to S_1 in the ground state, however, the particle was mainly localized on coordinated BF_2-core moiety. Therefore, the transition from S_0 to S_1 should contain a major part of π-π* featured transition with some contribution of CT transition from the electron-donor to the electron-acceptor. This was conducive to the formation of TICT fluorescence emission at 597 nm. Meanwhile, the hole was mainly delocalized on the TPA for the transition from S_1 to S_0 in the lowest singlet excited state, the particle was mainly localized on coordinated BF_2-core and partial TPA moieties. And the transition probability from S_1 to S_0 was higher than that from S_0 to S_1. Therefore, a LE state could be formed in the TPA moiety of the lowest singlet excited state. The corresponding fluorescence emission appeared at 460 nm.

2.4 AIE property

AIE activity of **PyTPABF$_2$** was explored due to the twisted configuration according to the result of molecular simulation. As shown in Figure 3(a), the emission intensity of **PyTPABF$_2$** in THF/water mixture with different water fraction (f_w referred to the volume percentage of water in mixtures) had distinct change. As shown in Figure 3(b), the

Table 2 Caclulated optimized conformation of **PyTPABF$_2$** in ground and excited states

	Ground state	Excited state
Optimized conformation	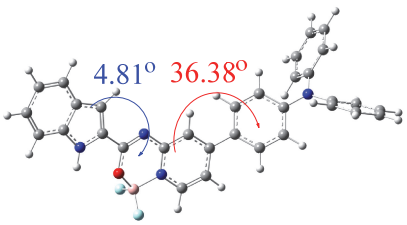	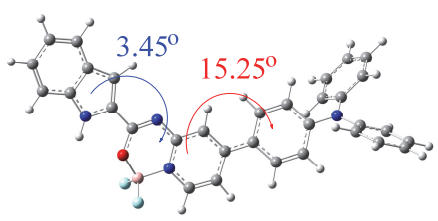

Table 3 Natural transition orbitals (NTO) for $S_0 \rightarrow S_1$ and $S_1 \rightarrow S_0$ transitions of **PyTPABF$_2$** in CH_3CN

Transition	Hole	Transition probability	Particle
$S_0 \rightarrow S_1$	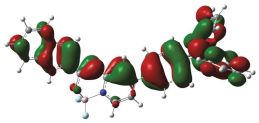	87.75 %	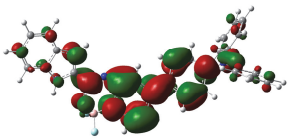
$S_0 \leftarrow S_1$	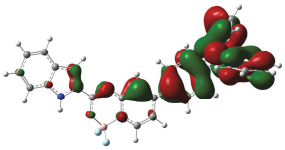	95.62 %	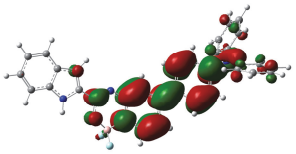

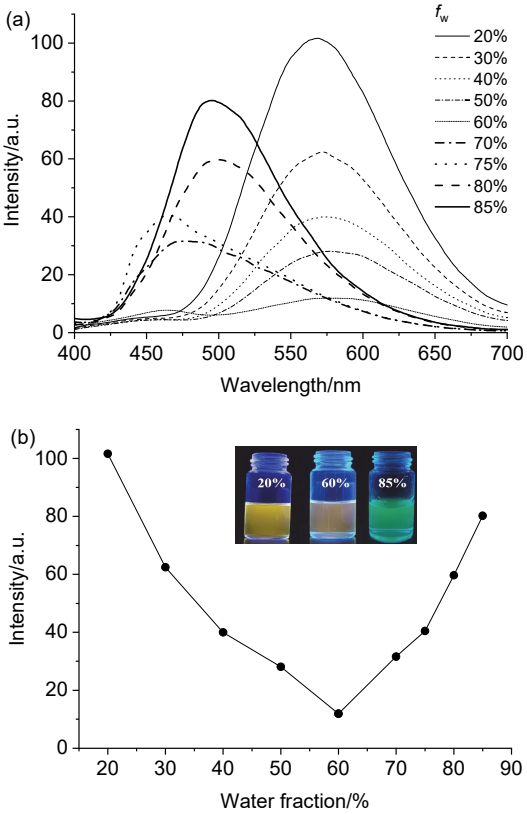

Figure 3 (a) Emission spectra of **PyTPABF$_2$** in THF/water mixtures with different water fractions (20%<f_w<85%), and (b) plots of emission peak intensity versus f_w in THF/water mixtures
Inset: photos in f_w irradiation 365 nm

emission intensity was gradually quenched and luminescence color also changed when f_w increasing from 20% to 60%. The TICT emission was further bule-shifted in the mixture solvent with 60% water, and the LE emission became apparent in the short wavelength region. A dual emission was observed. In the mixture solvent with 70% water, the LE emission became the only peak observed and the TICT peak in the long wavelength region disappeared.[21] When f_w increased to 85%, the emission intensity incrementally grew and solution emitted green light, suggesting that an aggregation state was formed due to increasing of f_w restriction intramolecular rotation and inhibition non-radiative transition. This phenomenon was called as AIE effect.

2.5 MFC property

As discussed above, **PyTPABF$_2$** with D-π-A conjugated twisted conformation had ICT characteristics and AIE property. This was demonstrated that it perhaps possessed MFC behavior. The luminescence color change was illustrated in Figure 4(a). The as-prepared solid powder of **PyTPABF$_2$** exhibited bright green light under 365 nm irradiation and the emission wavelength was located at 533 nm, which switched to khaki emitting powder with the emission wavelength red-shift to 556 nm upon grinding, the fluorescence quantum yield also decreased, and fluorescence lifetime (τ) had a slight longer than in the as-prepared state. In addition, the luminescence color in ground powder could recover to original color by fuming using CH_2Cl_2 vapor. Compared with the solid emission wavelength after grinding based on reported in the references, it was found that the red-shift values of difluoroboron compounds were relatively large besides **PyTPABF$_2$**. This could be related to the molecular structure, indicating that further exploring the relationship between molecular structure and MFC behaviors, was still one of the main directions of follow-up research. Moreover, multiple grinding and fuming cycles were exerted to **PyTPABF$_2$**. It was found that the MFC behaviors of **PyTPABF$_2$** displayed excellent reversibility.

To explore the mechanism of MFC behavior of **PyTPABF$_2$**, XRD patterns in different solid states were measured. As shown in Figure 4(b), the as-prepared powder displayed several sharp and intense diffraction peaks, indicating that the as-prepared powder of **PyTPABF$_2$** possessed an ordered arrangement. However, the diffraction peaks were very weak even disappeared after grinding, suggesting that the ground powder of **PyTPABF$_2$** had a disordered amorphous state due to mechanical force stimuli wrecking well-defined molecular packing.

Meanwhile, the diffraction peaks could be recovered through fuming the ground powder by using CH_2Cl_2 vapor, demonstrating that the amorphous state of the ground powder recovered to a crystalline state of the as-prepared powder. The above findings illustrated that the phase transformation between ordered arrangement and amorphous states was mainly responsible for MFC behavior of **PyT-**

PABF$_2$.

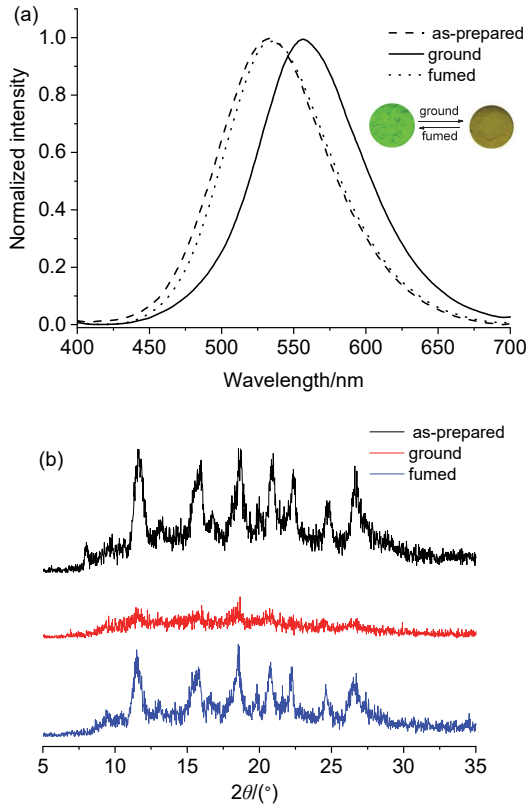

Figure 4 (a) Normalized fluorescence emission spectra (λ_{ex}= 365 nm) and (b) XRD patterns of **PyTPABF$_2$** in different solid states

Inset: photos in different solid states irradiation 365 nm

2.6 Data security property

The practical application of **PyTPABF$_2$** was further explored in ink-free rewritable paper for information encryption and decryption, according to its distinct chromatism by grinding-fuming process. A filter paper was immersed into 10 mL of CH_2Cl_2 of dissolving in 6 mg of pristine sample for 20 min, then the immersed filter paper was got out and dried at room temperature. The dried filter paper after soaking as security paper displayed green luminescence under 365 nm irradiation, immediately, the letter 'AQ' (abbreviation of Chinese Pinyin for "safe") was lightly crushed on the green background by using spatula, and 'AQ' emitted khaki light due to emission significantly red-shift under grinding (Figure 5). This was called the writing process. Afterwards, the letter 'AQ' could be erased after security paper fuming into CH_2Cl_2 vapor, which erasing process. Furthermore, two Chinese characters 'chemistry' were slightly crushed again, this was so-called rewriting process. And Chinese characters could be erased by fuming once again. It was illustrated that **PyTPABF$_2$** had a great potential application in data security protection.

3 Conclusions

In summary, a D-π-A type luminogen (**PyTPABF$_2$**) containing the electron-donor triphenylamine group and the electron-acceptor difluororboron moiety was successfully synthesized. The results revealed that **PyTPABF$_2$** exhibited apparent positive solvatochromism and excellent MFC performance. When the as-prepared powder was ground with a mortar and pestle, luminescent color switched from bright green light (533 nm) to khaki (556 nm). Meanwhile, it could be recovered reversibly after fuming by using CH_2Cl_2 vapor. XRD analysis revealed that phase transformation between crystalline and amorphous states was contributed to MFC behavior. More importantly, under external mechanical stimulation, the distinct chromatism of **PyTPABF$_2$** had been exploited fabricating security paper to achieve rewritable data storage.

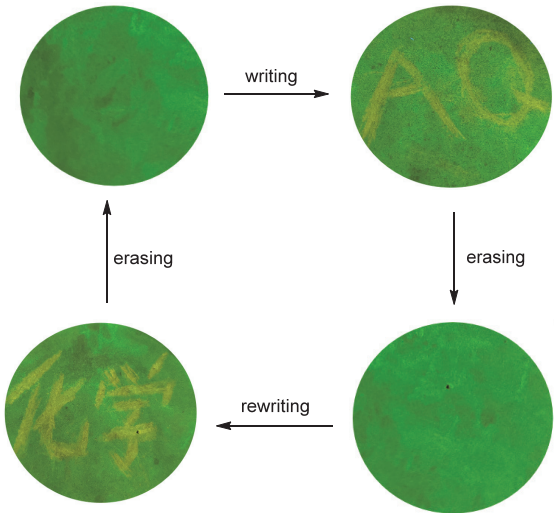

Figure 5 Photos of the luminescence rewriting process on the **PyTPABF$_2$**-loaded security paper under 365 nm irradiation

4 Experimental section

4.1 Instruments and reagents

The NMR spectra were recorded on a Bruker Advance II-400 spectrometer at 400, 375, and 101 MHz for ^{1}H NMR, ^{19}F NMR, and ^{13}C NMR spectra, respectively. Melt pointing were measured by an RY-1G melting point apparatus. High resolution mass spectrometry (HRMS) was obtained by a SCIEX X500 R Electrospray ionization-mass spectrometry for **PyTPABF$_2$** and a Aglient 6550 Q-TOF & Thermo Fisher-QW Electrospray ionization-mass spectrometry for **PyBr** and **PyTPA**. UV-vis spectra and fluorescence emission spectra were tested with a Shimadzu UV-2450 visible spectrophotometer and a Agilent carry eclipse fluorescence spectrophotometer, respectively. XRD patterns were obtained on a Bruker D2 phaser X-ray diffractometer. The calculation of **PyTPABF$_2$** was studied from the density functional theory (DFT) using M062X functional with 6-31G(d) as the basic set through the Gaussian 09 program package.

The dehydrated dichloromethane was obtained through reduced pressure distillation over CaH_2. Triethylamine (AR, 99%), 4-fluoronitrobenzene (98%), boron trifluoride diethyl

etherate (98%), 4-(diphenylamino)phenylboronic acid (98%), sodium bicarbonate, $Pd(PPh_3)_4$ and K_2CO_3 (Shanghai Macklin Bio-chem Technology Co. Ltd.) were used as received. All the other reagents and solvents were analytical grade, and they were used without further purification.

4.2 Synthesis

4.2.1 *N*-(4-Bromopyridin-2-yl)-1*H*-indole-2-carboxamide (**PyBr**)

A mixture of indole-2-carboxylic acid methyl ester (2.625 g, 15 mmol), 2-amino-4-bromopyridine (2.595 g, 15 mmol) and NaH (2.4 g, 99.9 mmol) in dehydrated THF (120 mL) was heated to 80 ℃ for 24 h under nitrogen atmosphere. After cooling to room temperature, the solvent was removed and saturated $NaHCO_3$ solution was added. The mixture was filtered, and the crude product was purified by column silica gel chromatography with CH_2Cl_2 as the eluent to obtain **PyBr**, 3.225 g, yield 68.1%. m.p. 240 ℃; ^{1}H NMR (400 MHz, DMSO-d_6) δ: 11.81 (s, 1H, pyrrole NH), 11.07 (s, 1H, amide NH), 8.51 (d, J=2.0 Hz, 1H, ArH), 8.33 (d, J=5.2 Hz, 1H, ArH), 7.67 (d, J=4.4 Hz, 2H, ArH), 7.50 (dd, J=8.4 Hz, 0.8 Hz, 1H, ArH), 7.45 (dd, J=5.6 Hz, 2.0 Hz, 1H, ArH), 7.27～7.23 (m, 1H, ArH), 7.10～7.06 (m, 1H, ArH); ^{13}C NMR (101 MHz, DMSO-d_6) δ: 160.76, 153.53, 149.72, 137.64, 133.52, 130.81, 127.45, 124.80, 122.99, 122.56, 120.54, 117.35, 112.94, 106.27; HRMS calcd for $C_{14}H_{10}BrN_3O$ 316.0085, found 316.0071.

4.2.2 *N*-(4-(4-(Diphenylamino)phenyl)pyridin-2-yl)-1*H*-indole-2-carboxamide (**PyTPA**)

A mixture of **PyBr** (0.474 g, 1.5 mmol), 4-(diphenylamino)phenyl boronic acid (0.5 g, 1.7 mmol), $Pd(PPh_3)_4$ (0.1 g, 0.08 mmol) and K_2CO_3 (0.5 g, 3.6 mmol) in toluene (30 mL) and distilled water (15 mL) was heated to 100 ℃ for 20 h under nitrogen atmosphere. The mixture was extracted by CH_2Cl_2 (30 mL×3) and organic solvent was removed, then the crude product was purified by column silica gel chromatography with CH_2Cl_2 as the eluent to obtain **PyTPA**, 0.23 g, yield 31.9%. m.p. 248 ℃; ^{1}H NMR (400 MHz, DMSO-d_6) δ: 11.78 (s, 1H, pyrrole NH), 10.85 (s, 1H, amide NH), 8.51 (d, J=0.8 Hz, 1H, ArH), 8.42 (d, J=5.2 Hz, 1H, ArH), 7.72～7.64 (m, 4H, ArH), 7.50 (d, J=8.0 Hz, 1H, ArH), 7.45 (dd, J=5.2 Hz, 1.6 Hz, 1H, ArH), 7.38 (t, J=8.4 Hz, 4H, ArH), 7.26 (t, J=8.0 Hz, 1H, ArH), 7.14～7.06 (m, 9H, ArH); ^{13}C NMR (101 MHz, DMSO-d_6) δ: 160.61, 153.28, 149.03, 148.96, 148.94, 147.18, 137.52, 131.31, 131.03, 130.22, 128.33, 127.53, 125.26, 124.58, 124.31, 122.78, 122.46, 120.46, 117.27, 112.90, 111.53, 105.79; HRMS calcd for $C_{32}H_{24}N_4O$ 481.2028, found 481.2015.

4.2.3 4-(1,1-Difluoro-3-(1*H*-indol-2-yl)-1*H*-1λ^4,9λ^4-pyrido[1,2-*c*][1,3,5,2]oxadiazaborinin-6-yl)-*N*,*N*-diphenylaniline (**PyTPABF$_2$**)

PyTPA (0.48 g, 1.0 mmol) reacted with BF_3•Et_2O (1 mL, 7.9 mmol) in the presence of triethylamine (1.0 mL, 7.2 mmol) in dehydrated CH_2Cl_2 (20 mL), and the solution was stirred under atmosphere for 24 h. The mixture was extracted successively by saturated $NaHCO_3$ (60 mL×2) solution and CH_2Cl_2 (30 mL×3), and organic solvent was removed. Then the crude product was purified by column silica gel chromatography with CH_2Cl_2 as the eluent to obtain **PyTPABF$_2$**, 0.32 g, yield 60.3%. m.p. 322 ℃; ^{1}H NMR (400 MHz, DMSO-d_6) δ: 12.01 (s, 1H, pyrrole NH), 8.46 (d, J=6.4 Hz, 1H, ArH), 7.95 (d, J=8.8 Hz, 2H, ArH), 7.90 (dd, J=6.4 Hz, 2.0 Hz, 1H, ArH), 7.75 (d, J=1.6 Hz, 1H, ArH), 7.70 (d, J=8.0 Hz, 1H, ArH), 7.53 (dd, J=8.4 Hz, 0.8 Hz, 1H, ArH), 7.44～7.40 (m, 5H, ArH), 7.31～7.26 (m, 1H, ArH), 7.23～7.18 (m, 6H, ArH), 7.12～7.08 (m, 1H, ArH), 7.02(d, J=8.8 Hz, 2H, ArH); ^{13}C NMR (101 MHz, DMSO-d_6) δ: 159.32, 154.89, 153.81, 150.89, 146.48, 139.53, 138.76, 130.50, 130.44, 129.35, 127.77, 127.73, 126.48, 126.32, 125.54, 125.36, 122.51, 120.84, 120.68, 118.29, 117.51, 113.21, 109.26; ^{19}F NMR (376 MHz, DMSO-d_6) δ: −137.16, −137.23; HRMS calcd for $C_{32}H_{23}BF_2N_4O$ 529.1967, found 529.2000.

Supporting Information ^{1}H NMR and ^{13}C NMR spectra of indole-2-carboxylic acid methyl ester, **PyBr**, **PyTPA** and **PyTPABF$_2$**; ^{19}F NMR spectrum of **PyTPABF$_2$**; HRMS spectra of **PyBr**, **PyBrTPA** and **PyTPABF$_2$**; repeated fluorescence switch of **PyTPABF$_2$** by grinding and fuming cycles; photophysical data of **PyTPABF$_2$** in different polarity organic solvent and solid-state; the reported paper involving MFC data of in references. The Supporting Information is available free of charge via the Internet at http://sioc-journal.cn/.

References

[1] Li, Z.; Chen, H.; Li, B.; Xie, Y.; Gong, X.; Liu, X.; Li, H.; Zhao, Y. *Adv. Sci.* **2019**, *21*, 1901529.

[2] Wu, Z.; Du, B.; Tong, G.; Zhang, H.; Zhang, Y.; Xia, J.; Zhao, Z. *Chem. Eng. J.* **2022**, *428*, 131016.

[3] Lu, L.; Wang, K.; Wu, H.; Qin, A.; Tang, B. Z. *Chem. Sci.* **2021**, *12*, 7058.

[4] Yan, N.; Zhang, W.; Li, G.; Zhang, S.; Yang, X.; Zhou, K.; Pei, D.; Zhao, Z.; He, G. *Mater. Chem. Front.* **2021**, *5*, 4128.

[5] Ma, Y.; Zhang, Y.; Kong, L.; Yang, J. *Molecules* **2018**, *12*, 3255.

[6] Hu, J.; Wang, J.; Liu, R.; Li, Y.; Lu, J.; Zhu, H. *Dyes Pigm.* **2018**, *153*, 84.

[7] Fu, S.; Feng, X.; Zhou, N.; Zhang, S.; Liu, X.; Xu, D. *J. Lumin.* **2022**, *247*, 118802.

[8] Pannipara, M.; Al-Sehemi, A. D.; Kalam, A.; Asiri, A. M. *Opt. Mater.* **2017**, *72*, 442.

[9] Song, Z.; Liu, R.; Li, Y.; Shi, H.; Hu, J.; Cai, X.; Zhu, H. *J. Mater. Chem. C* **2016**, *4*, 2553.

[10] Zhang, H.; Chen, P.-Z.; Niu, L.-Y.; Yang, Q.-Z. *Mater. Chem. Front.* **2020**, *4*, 285.

[11] Saotome, S.; Suenaga, K.; Tanaka, K.; Chujo, Y. *Mater. Chem. Front.* **2020**, *4*, 1781.

[12] Nandi, R. P.; Sudhakar, P.; Kalluvettukuzhy, N. K.; Thilagar, P. *Chem.-Eur. J.* **2020**, *69*, 16306.

[13] Sun, J.; Yang, H.; Simalou, O.; Lv, K.; Zhai, L.; Zhao, J.; Lu, R. *New J. Chem.* **2019**, *43*, 10134.

[14] Li, P.; Liang, Q.; Hong, E. Y.-H.; Chan, C.-Y.; Cheng, Y.-H.; Leung, M.-Y.; Chan, M.-Y.; Low, K.-H.; Wu, H.; Yam, V. W.-W. *Chem. Sci.* **2020**, *42*, 11601.

[15] Kuno, A.; Tohnai, N.; Yasuda, N.; Maeda, H. *Chem.-Eur. J.* **2017**,

47, 11357.
[16] Kubota, Y.; Niwa, T.; Jin, J.; Funabiki, K.; Matsui, M. *Org. Lett.* **2015**, *12*, 3174.
[17] Kubota, Y.; Sakuma, Y.; Funabiki, K.; Matsui, M. *J. Phys. Chem. A* **2014**, *38*, 8717.
[18] Michalsky, I.; Gensch, V.; Walla, C.; Hoffmann, M.; Rominger, F.; Oeser, T.; Tegder, P.; Dreuw, A.; Kivala, M. *Chem.-Eur. J.* **2022**, *34*, e202200326.
[19] Tu, J.; Fan, Y.; Wang, J.; Li, X.; Liu, F.; Han, M.; Wang, C.; Li, Q.; Li, Z. *J. Mater. Chem. C* **2019**, *39*, 12256.
[20] Aleveque, O.; Achelle, S.; Sanguient, L. *ChemPhotoChem* **2023**, *7*, e202200201.
[21] Hu, R.; Lager, E.; Aguilar-Aguilar, A.; Liu, J.; Lam, J. W. Y.; Sung, H. H. Y.; Williams, I. D.; Zhong, Y.; Wong, K. S.; Pena-Cabrera, E.; Tang, B. Z. *J. Phys. Chem. C* **2009**, *36*, 15845.

(Cheng, F.)

